OFF-DESIGN ANALYSIS OF ORGANIC RANKINE CYCLE INTEGRATED WITH PROTON EXCHANGE MEMBRANE FUEL CELL

Hong Wone Choi[1], Jin Young Park[1], Dong Kyu Kim[2], Min Soo Kim[1]*

[1]Department of Mechanical and Aerospace Engineering, Seoul National University
Seoul, Republic of Korea
hongone90@snu.ac.kr, zeragon@snu.ac.kr, minskim@snu.ac.kr*

[2]School of Mechanical Engineering, Chung-Ang University
Seoul, Republic of Korea
dkyukim@cau.ac.kr

* Corresponding Author

ABSTRACT

The primary target of this study is to examine performance shift during off-design operation of a proton exchange membrane fuel cell (PEM fuel cell). Recently, an organic Rankine cycle (ORC) system has been considered to improve the energy efficiency of the PEM fuel cell system through recovering waste heat from a fuel cell stack. However, due to deterioration of fuel cell or change of operating conditions, a heat source temperature of the ORC system which influence the performance of the ORC system can be varied. A key question of this research is, thus, how the performance of the hybrid system changes from a design point of PEM fuel cell concerning a variation of temperature and mass flow rate of coolant of the fuel cell system. To investigate the off-design performance of the ORC system, mathematical models of the ORC system and PEM fuel cell are set up under a steady-state regime. As a result, the amount of heat played a more significant role in ORC performance when the evaporator size was enough to absorb the waste heat of fuel cell stack. The fuel cell performance decreased with a rise of cell temperature, however, the bottoming ORC system compensated for the deterioration of fuel cell.

1. INTRODUCTION

With the development of modern society, the consumption of fossil fuel has gradually increased year by year. The increase of fossil fuel usage has accelerated depletion of energy resources and has raised several environmental issues; global warming, severe air pollution and so on. To properly handle these global issues and achieve sustainable development of modern society, many eco-friendly energy technologies have emerged as alternatives to fossil fuel. In some developed countries, PEM fuel cell can be considered as power source which can be widely used to fulfill energy demand from transportation to household.

Generally, the energy efficiency of a PEM fuel cell is regarded as about 50% because PEM fuel cell releases waste heat equivalent to its electric power output [1]. As a strategy of waste heat recovery (WHR), many researchers have suggested combined heat and power (CHP) system which can provide not only electric power but also hot water. Currently, the CHP system has already approached to the commercialization stage [2]. CHP system effectively exploits thermal energy from fuel cell coolant by directly using hot water. However, the usage of heating or hot water could be restrictive depending on seasonal effects. Therefore, this WHR strategy can be limited.

Whereas WHR strategy using ORC to produce useful power is rarely affected by season changes, so it stably enhance the energy efficiency of the power system regardless of seasonal effects. Zhao et al. (2012) proposed a combined hybrid power system that a bottoming ORC recovers waste heat from PEM fuel cell [3]. Sheshpoli et al. (2018) designed several system layouts of the hybrid power system which

exploits not only waste heat of fuel cell stack but also waste heat from auxiliaries such as compressor and hydrogen preheater [4]. The previous studies conducted focused on proposing hybrid power systems. However, the studies in the past rarely considered the temperature effect which is a critical variables to both fuel cell thermal management system and the ORC system.

PEM fuel cell operates at its optimal point usually around cell temperature of 343 K. In reality, PEM fuel cell experiences deterioration or change of operating condition, and this can cause a change of fuel cell temperature or the amount of waste heat, i.e., meaning a change of heat source condition of a bottoming ORC. In this study, we investigated the performance shift of ORC system concerning changes in fuel cell temperature from fuel cell operation of 343 K.

2. SYSTEM DESCRIPTION

The hybrid power system consists of 10 kW PEM fuel cell and the bottoming ORC as shown in Figure 1. Humidified air and hydrogen fuel are injected to cathode and anode of the fuel cell stack, respectively. Through an electrochemical reaction between hydrogen and oxygen, electric power is generated and also waste heat is released because of the losses during operation. The evaporator connects two different power system, PEM fuel cell, and ORC. Waste heat generated from fuel cell stack is transferred to the evaporator by stack coolant. A brazed plate heat exchanger is used for the evaporator and condenser. Refrigerant R245fa, circulating the ORC system, is vaporized by getting thermal energy. Passing through the expander, the refrigerant vapor generates additional power.

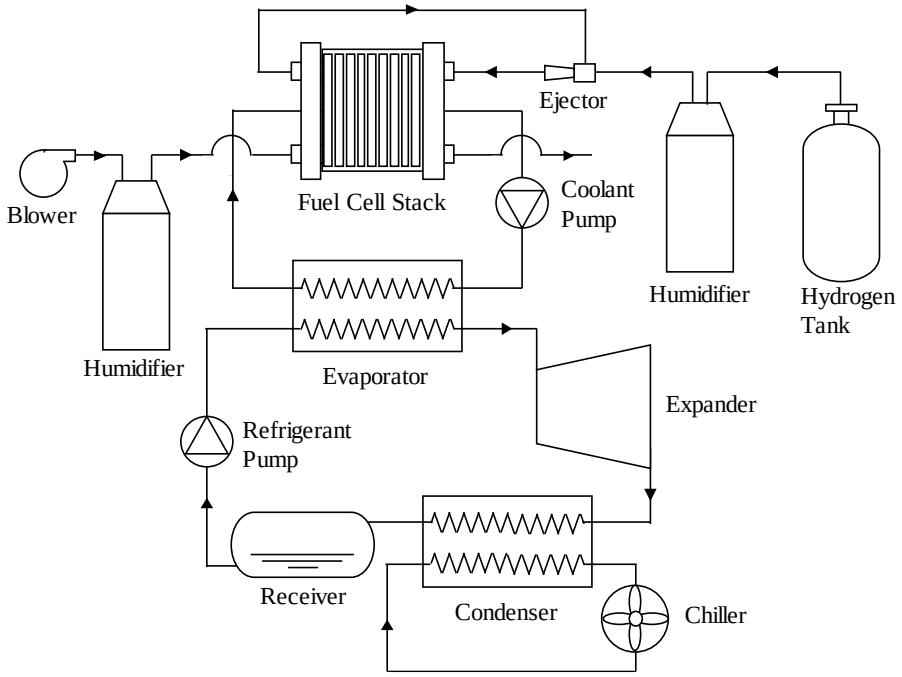

Figure 1: Schematic diagram of PEM fuel cell-bottoming ORC system

3. MATHEMATICAL MODEL

3.1 Simulation conditions

Several assumptions were made to simplify the simulation model:

(1) The system operates under a steady-state regime
(2) The reactants of the fuel cell are humidified to 100%.
(3) Temperature of the exhausted from the stack is assumed to be equivalent to stack temperature.
(4) Temperature difference of gas and coolant between stack's inlet and outlet is kept at 5 K.
(5) The hybrid system operates on the temperature which the bottoming ORC can fully cool down the fuel cell stack.

Table 1: Operating conditions of the hybrid power system

Parameter Bottom	Symbol	Value	Unit
Operating current density of stack	j	0.9	A/cm^2
Operating cell temperature	T_{cell}	343 ~ 353	K
Pressure at anode/cathode	P_{an}/P_{ca}	104/117	kPa
Stoichiometric number of hydrogen/air	λ_{H2} /λ_{air}	1.5/2.0	-
Mass flow rate of refrigerant	$\dot{m}_r$	0.02 ~ 0.03	kg/s
Temperature of cold water at the condenser inlet	T_{cw}	298	K
Mass flow rate of cold water at the condenser	$\dot{m}_{cw}$	0.35	kg/s

(6) Pressure drop in fuel cell channel, pipe and heat exchanger is negligible.
(7) Heat loss to ambient air is negligible.
(8) Ambient temperature is 298 K.
(9) Degree of subcooling (DSC) of ORC is continuously kept at 9 K.
(10) Isentropic efficiencies of pump and expander are constant regardless of operating condition.
(11) The electrical conversion efficiencies of pump and expander are 100%.

Mass flow rate of the bottoming ORC was adjusted to get waste heat carried by stack coolant fully following change of cell temperature. The simulation model operated in the following conditions as presented in Table 1. Empirical values suggested in fuel cell fundamentals were adopted as design parameters of PEM fuel cell model [5]. Design parameters of ORC are set up based on ORC test rig. Table 2 depicts the design parameters and empirical values of the hybrid system. The simulation model is executed in Matlab. REFPROP ver.9.1 made by NIST provided fluid properties of the working fluids in the simulation model.

3.2 PEM Fuel Cell Model

Based on thermodynamic principles, a PEM fuel cell model was set up under the steady-state regime. Governing equation of PEM fuel cell based on energy conversance law is as follows;

$$\dot{Q}_{chem} - \dot{W}_{st} - (\dot{Q}_{coolant} + \dot{Q}_{gas}) = 0 \quad (1)$$

Where $\dot{Q}_{chem}$ is chemical heat from electrochemical reaction and obtained from a high heating value (HHV) of water forming reaction as shown in Eq. (2).

Table 2: Design parameters of the hybrid system

Parameter	Symbol	Value	Unit
Number of cells of the stack	N_{cell}	50	-
Active area of cell	A_{cell}	200	cm^2
Exchange current density of the anode	$J_{0,an}$	0.1	A/cm^2
Exchange current density of the cathode	$J_{0,ca}$	10^{-4}	A/cm^2
Transfer coefficient of the anode	α_{an}	0.5	-
Transfer coefficient of the cathode	α_{ca}	0.3	-
Area specific resistance of the cell	ASR	0.01	Ω·cm^2
Limiting current density	j_L	2	A/cm^2
Concentration overpotential constant	c	0.1	V
Pump efficiency	η_p	0.4	-
Isentropic efficiency of expander	η_t	0.8	-
Heat transfer area of the evaporator	A_{evap}	780	cm^2
Number of a plate of the evaporator	N_{evap}	32	-
Heat transfer area of the condenser	A_{cond}	471	cm^2
Number of a plate of the condenser	N_{cond}	50	-

$$\dot{Q}_{chem} = \dot{n}_{H_2,rxn} \Delta\hat{h}_{HHV} \quad (2)$$

HHV denoted as $\Delta\hat{h}_{HHV}$, is -286 kJ/mol and molar flow rate of hydrogen required for the reaction is calculated with Eq. (3).

$$\dot{n}_{H_2,rxn} = \frac{N_{st}\, I_{st}}{nF} \quad (3)$$

F is Faraday's constant, 96485 C/mol. n is the molar number of electron transferred during the reaction. For hydrogen, n is referred to 2, meanwhile 4 for oxygen. In the same manner, molar flow rate of oxygen consumed during the reaction and water formed by the reaction can be obtained. Electric power of fuel cell stack is:

$$\dot{W}_{st} = N_{cell}\, V_{cell} I_{st} \quad (4)$$

Operating cell voltage can be obtained by taking three types of overpotential into account. A governing equation determining cell voltage is as follows;

$$V_{cell} = E_{Nernst} - V_{act} - V_{ohm} - V_{conc} \quad (5)$$

Where E_{Nernst} is the thermodynamic potential of fuel cell and the others are overpotential, i.e. voltage loss. Empirical equation is used for calculating the thermodynamic potential [6].

$$E_{Nernst} = 1.229 - 8.5 \times 10^4 (T_{cell} - 298.15) + 4.308 \times 10^5 \times T_{cell} (ln\, P_{H_2} + 0.5\, ln\, P_{O_2}) \quad (6)$$

According to the Butler-Volmer equation, activation overpotential is:

$$V_{act} = -\frac{RT_{cell}}{\alpha nF} ln\, j_0 + \frac{RT_{cell}}{\alpha nF} ln\, j \quad (7)$$

Ohmic loss on the membrane cell is:

$$V_{ohm} = ASR \times j \quad (8)$$

Where ASR is an abbreviated word of area specific resistance. Concentration overpotential caused by slowness in mass transport is:

$$V_{conc} = c\, ln \frac{j_L}{j_L - (j + j_{leak})} \quad (9)$$

Based on energy conservation law, heat dissipation with the gas exhaust is obtained by comparing heat carried by both intake and exhaust.

$$\dot{Q}_{gas} = \dot{Q}_{st,o} - \dot{Q}_{st,i} \quad (10)$$

Consequently, heat removal by the coolant is obtained from the above Eq. (1).

3.3 ORC Model

Thermodynamic model of single loop ORC system was set up. Pump frequency is adjusted until convective heat transfer at the evaporator is equivalent to heat dissipation of fuel cell by its coolant. Power consumption of pump is calculated from hydraulic power and .pump efficiency.

$$\dot{W}_p = \frac{\Delta P \dot{m}_r}{\rho_r \eta_p} \quad (11)$$

Effectiveness-NTU method was adopted to calculate the amount of convective heat transfer. Desideri et al. (2017) studied a correlation of the boiling heat transfer coefficient of R245fa in the brazed plate heat exchanger, and the proposed correlation Eq. (12) is selected to the ORC model [7].

$$h_{bo} = 1.48 \times 10^3 \, We^{-3.22e-2} \left(\frac{\rho_l}{\rho_v}\right)^{-3.38e-1} Re_l^{4.51e-1} Bd^{-4.69e-1} \tag{12}$$

The power output of the expander is:

$$\dot{W}_{exp} = \dot{m}_r (i_i - i_o)_{exp} \tag{13}$$

Correlation equation of condensing heat transfer suggested by Yan et al. (1999) was used to obtain the amount of heat transfer at the condenser [8].

$$Nu_{co} = 4.118 \, Re_{eq}^{0.4} Pr_l^{0.3} \tag{14}$$

One of the essential performance criteria, the thermal efficiency of the bottoming ORC, is obtained by comparing net power versus heat input to the evaporator.

4. RESULTS

The ORC simulation model was verified by comparing with the experimental data as depicted in figure 2. The points and lines represent the experimental data and the simulation results, respectively. As shown in the figure 2(a), power output of the expander and heat input to the evaporator were measured with respect to varying mass flow rate when temperature of heat source and heat sink was constant as 353 and 293K, respectively. The experimental data were measure when a superheated vapor is injected to the expander. Based on pump affinity laws, pump head, i.e. pumping pressure, increases proportional to square of rotational speed of pump. In this reason, the increase of mass flow rate caused the increase of the pressure ratio between the expander inlet and outlet, and the rise of the pressure ratio enhanced the power output from the expander. In terms of the accuracy of the simulation model in power output, the simulation results mostly placed in ±10% errors as shown in the figure 2(b). Heat input to the evaporator increased with mass flow rate because the rise of Reynold number enhanced the heat transfer coefficient.

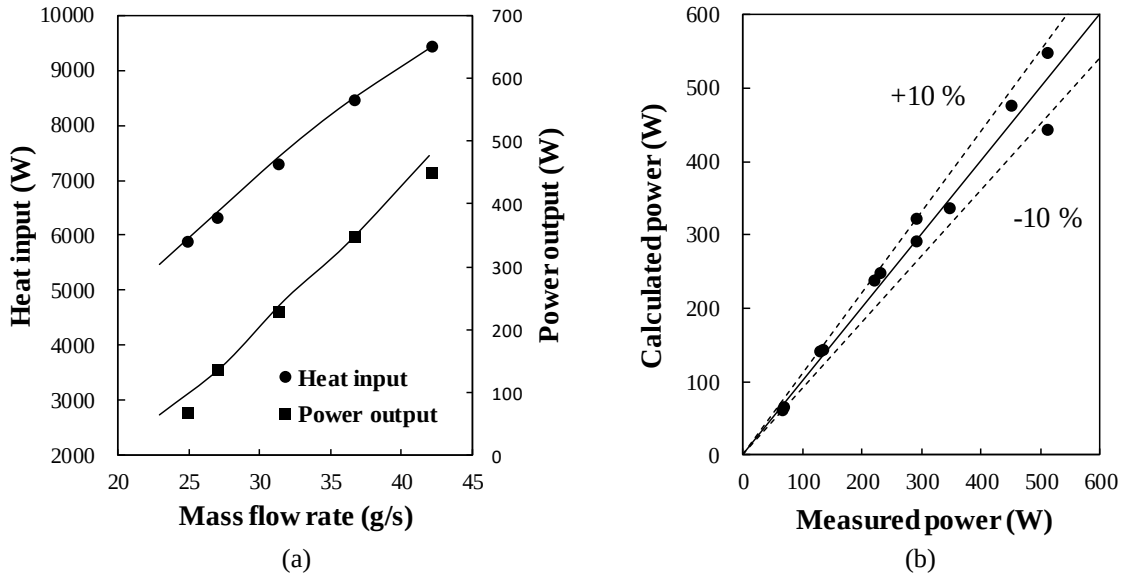

Figure 2: Validation for the ORC simulation model (a), accuracy of the simulation model (b)

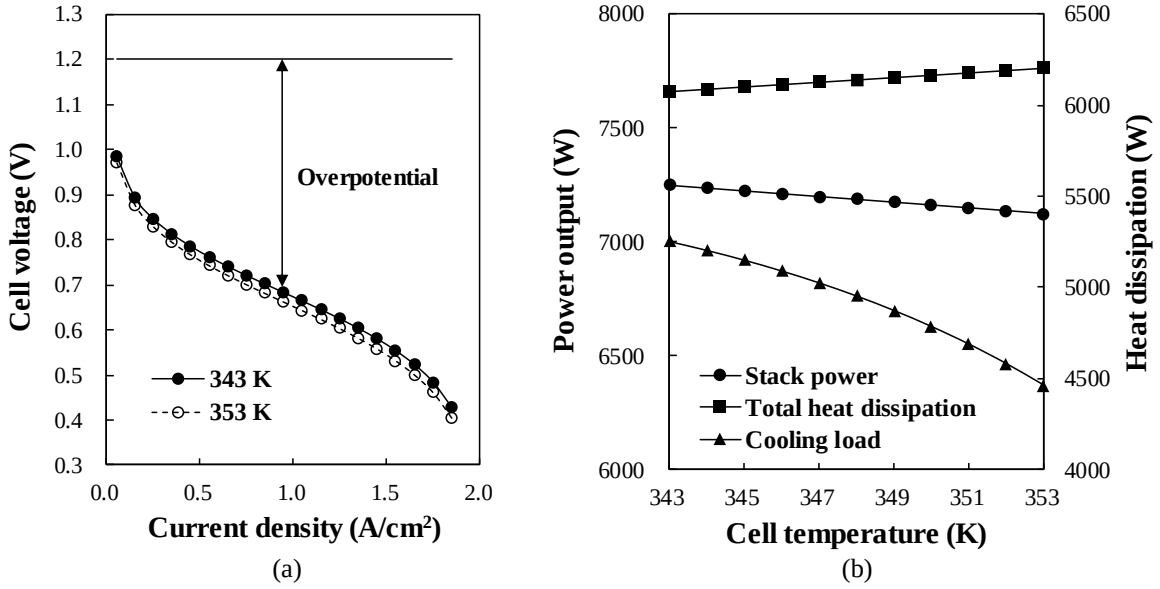

Figure 3: Cell voltage (a), power output and waste heat (b) of fuel cell stack

With respect to the change of cell temperature, the simulation study was conducted at the fixed operating current density of fuel cell stack. Figure 3 represents the performance of fuel cell stack with respect to cell temperature and operating current density. With increasing operating current density of fuel cell ohmic and concentration overpotential, respectively, and the amount of overpotential acted on the fuel cell was sequentially affected by activation, ohmic and concentration overpotential, respectively, and the amount of overpotential acted on the fuel cell was cumulated. The overall overpotential can be expressed as the difference between ideal thermodynamic potential and cell voltage as depicted in the figure 3(a). The increment of the overall overpotential means the fuel cell losses much more energy as a form of waste heat. Comparing two operating cases where the cell temperature is 343K, 353K in the figure 3(a), with the increment of cell temperature, the stack released more waste heat where the operating current density is constant. The figure 3(b) shows power output and heat dissipation of stack with respect to stack's cell temperature when operating current density is 0.9 A/cm^2. The value of current density was determined where the evaporator of the bottoming ORC can fully accept the waste heat from the stack under steady state. The power output of stack decreased with temperature increase, whereas the total amount of heat dissipation increased due to the overpotential increment. However, cooling load meaning the heat dissipation by stack coolant decreased with temperature. This is because

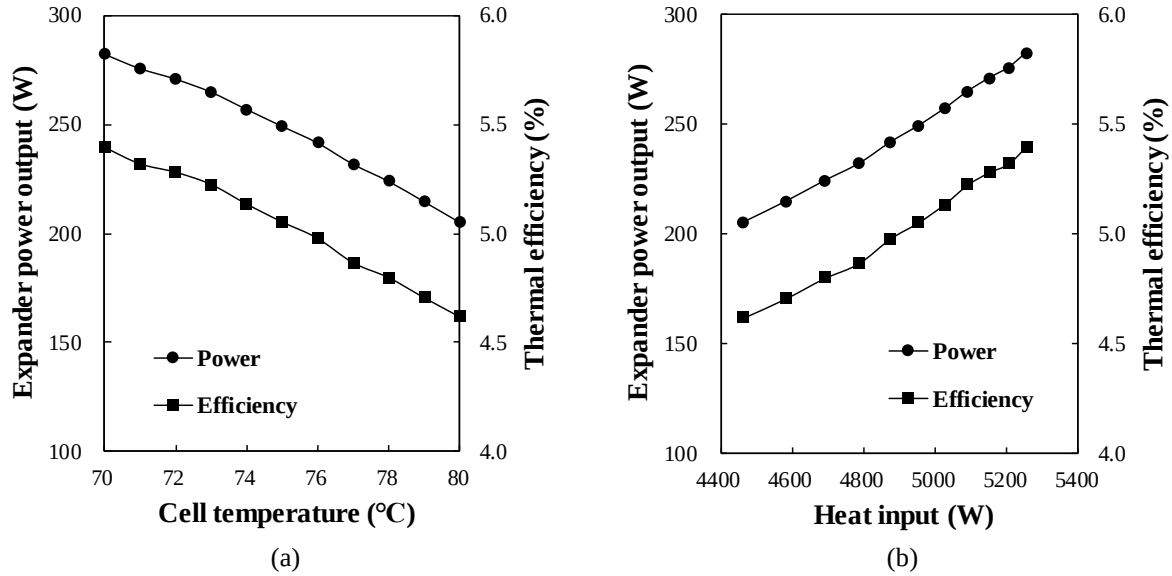

Figure 4: Performance of the bottoming ORC with regard to cell temperature (a), heat input (b)

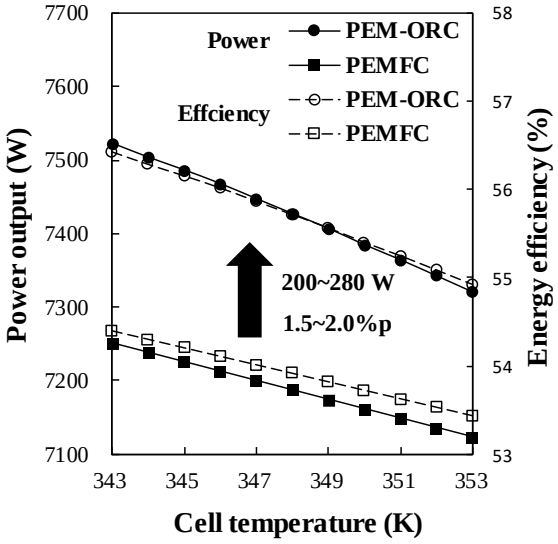

Figure 5: Performance enhancement of the PEM-ORC hybrid power system

moisture contents of gas exit from fuel cell's cathode increase with operating temperature increase, thus a part of waste heat is consumed as latent heat as the number of water contents [9]. In this reason, heat input provided to the evaporator of the bottoming ORC decreased with temperature increase.

Figure 4 shows the performance of the bottoming ORC with respect to the operating condition of the PEM fuel cell. As mentioned above, it is assumed that the hybrid system operates where the bottoming ORC can fully cool down waste heat from the stack by itself. In the figure 4(a), even though cell temperature, that is heat source temperature to the bottoming ORC, increased, expander's power output and thermal efficiency of the ORC decreased. Whereas, the increase of heat input meaning cooling load of fuel cell stack enhanced both performance indicators. Although cell temperature rises, the expander cannot accomplish better performance. The low heat input restricted the bottoming ORC pumping the more working fluid.

Performance enhancement of the PEM-ORC hybrid power systems is described in the figure 5. By recovering waste heat of fuel cell stack, the hybrid power system obtained about 200 to 280 W additional power, and those are equivalent to energy efficiency enhancement of 1.5~2.0%p. With the increase of operating temperature of fuel cell from 343K, performances of fuel cell were deteriorated. However, when comparing performances of the hybrid system operating in 353K and those of PEM fuel cell operating in 343K, the bottoming ORC compensated the performance degradation caused due to the increase of the operating cell temperature.

5. CONCLUSIONS

Off-design characteristics of the hybrid power system were studied with regard to the change of cell temperature and waste heat dissipation. The results showed that heat input to the evaporator decreased with increasing cell temperature from the ordinary temperature of 343 K. The amount of heat played a more significant role in ORC performance when the evaporator size was sufficient to absorb the whole volume of waste heat. The cooling load reduction caused performance degradation of the bottoming ORC, although coolant temperature increased.

In terms of an overall power output and energy efficiency of the hybrid power system, the bottoming ORC generated additional power as the amount of 200 to 280 W. The power output range of the hybrid power system shifted from the range of about 7,100 ~ 7,251 W to 7,321 ~ 7,523 W. Also, the energy efficiency of the hybrid system was enhanced as about 1.5 to 2.0%p from that of PEM fuel cell only. Furthermore, it was shown that the bottoming ORC can compensate power degradation of fuel cell stack due to temperature rise. The power output of the hybrid system at 353 K was higher as 70 W than that of fuel cell stack at 343 K. The ORC can be a solution to alleviate the effect of fuel cell deterioration.

NOMENCLATURE

n	molar flow rate	(mol/s)
N	number	(-)
j	current density	(A/cm^2)
i	enthalpy	(J/kg·K)
h	heat transfer coefficient	($W/m^2·K$)
ρ	density	(kg/m^3)
We	Weber number	(-)
Bd	Bond number	(-)

Subscript

st	stack
ad	anode
ca	cathode
L	limiting
i	inlet
o	outlet
bo	boiling
co	condensing
eq	equivalent
r	refrigerant
l	liquid
v	vapor

REFERENCES

[1] Kandlikar, S. G. and Lu, Z., 2009, Thermal Management Issues in a PEMFC Stack – A Brief Review of Current Status, *Appl. Therm. Eng.*, vol. 29, no. 7: pp. 1276-1280

[2] Sharaf, O. Z. and Orhan, M. F., 2014, An Overview of Fuel Cell Technology: Fundamentals and Applications, *Renew. Sust. Energ. Rev.*, vol. 32, pp. 810-853

[3] Zhao, P., Wang, J., Gao, L., and Dai, Y., 2012, Parametric Analysis of a Hybrid Power System Using Organic Rankine Cycle to Recover Waste Heat from Proton Exchange Membrane Fuel Cell, *Int. J. Hydrogen Energ.*, vol. 37, no. 4: pp. 3382-3391

[4] Sheshpoli, M. A., Ajarostaghi, S. S. M., and Delavar, M. A., 2018, Waste Heat Recovery from a 1180 kW Proton Exchange Membrane Fuel Cell (PEMFC) System by Recuperative Organic Rankine Cycle (RORC), *Energy*, vol. 157, pp. 353-366

[5] O'hayre, R., Cha, S.-W., Colella, W. G., and Prinz, F. B., 2016, *Fuel Cell Fundamentals*, John Wiley & Sons, New Jersey, 222 p.

[6] Zhao, X., Li, Y., Liu, Z., Li, Q., and Chen, W., 2015, Thermal Management System Modeling of a Water-Cooled Proton Exchange Membrane Fuel Cell, *Int. J. Hydrogen Energ.*, vol. 40, no. 7: pp. 3048-3056

[7] Desideri, A., Zhang, J., Kærn, M.R., Ommen, T.S.,Wronski, J., Lemort, V. and Haglind, F., 2017, An Experimental Analysis of Flow Boiling and Pressure Drop in a Brazed Plate Heat Exchanger for Organic Rankine Cycle Power Systems, *Int. J. Heat. Mass. Tran.*, vol. 113, pp. 6-21

[8] Yan, Y. Y., Lio, H. C., and Lin, T. F., 1999, Condensation Heat Transfer and Pressure Drop of Refrigerant R-134a in a Plate Heat Exchanger, *Int. J. Heat. Mass. Tran.*, vol. 42, no. 6: pp. 993-1006

[9] Mallant, R. K. A. M., 2003, PEMFC Systems: The Need for High Temperature Polymers as a Consequence of PEMFC Water and Heat Management, *J. Power Sources*, vol. 118, no. 1: pp. 424-429